Tuning the Terahertz Emission Power of an Intrinsic Josephson-Junction Stack with a Focused Laser Beam

X. J. Zhou,[1,2,3] J. Yuan,[4] H. Wu,[2,5] Z. S. Gao,[2] M. Ji,[1,2] D. Y. An,[1] Y. Huang,[1] F. Rudau,[6] R. Wieland,[6] B. Gross,[6] N. Kinev,[7] J. Li,[1] A. Ishii,[2] T. Hatano,[2] V. P. Koshelets,[7] D. Koelle,[6] R. Kleiner,[6] H. B. Wang,[1,2,3,*] and P. H. Wu[1]

[1]*Research Institute of Superconductor Electronics, Nanjing University, Nanjing 210093, China*
[2]*National Institute for Materials Science, Tsukuba 3050047, Japan*
[3]*Cooperative Innovation Centre of Terahertz Science, Chengdu 610054, China*
[4]*National Lab for Superconductivity, Institute of Physics, Chinese Academy of Sciences, Beijing 100190, China*
[5]*Key Laboratory of Artificial Micro- and Nano-Structures of Ministry of Education, School of Physics and Technology, Wuhan University, Wuhan 430072, China*
[6]*Physikalisches Institut and Center for Collective Quantum Phenomena in LISA+, Universität Tübingen, D-72076 Tübingen, Germany*
[7]*Kotel'nikov Institute of Radio Engineering and Electronics, Moscow 125009, Russia*

(Received 5 February 2015; revised manuscript received 1 April 2015; published 21 April 2015)

We report on tuning the THz emission of a $Bi_2Sr_2CaCu_2O_8$ (BSCCO) intrinsic Josephson-junction stack by a focused laser beam which is scanned across the stack. The emission power P_e increases by up to 75% upon laser irradiation for a bath temperature near 22 K. The laser-induced changes in the voltage V_{dc} across the stack and in the emission power are measured simultaneously. The maximum of the laser-induced changes in emission power ΔP_e is achieved by irradiating the stack on the location where the local temperature is about the critical temperature T_c. However, ΔP_e is found to be proportional to the laser-induced global voltage change ΔV_{dc}, irrespective of the laser position. This unexpected *global* response is likely to be related to a change in the *average* stack temperature and is consistent with the change in P_e when increasing the bath temperature by about 0.2 K. This tuning method can be employed in the application of BSCCO THz sources.

DOI: 10.1103/PhysRevApplied.3.044012

I. INTRODUCTION

Developing compact, tunable sources for THz generation is a highly active field of research [1,2]. Recently, it was found that intrinsic Josephson-junction (IJJ) stacks, naturally formed in the cuprate superconductor $Bi_2Sr_2CaCu_2O_8$ (BSCCO), can emit coherent radiation at submillimeter wavelengths [3]. In Ref. [3], stacks consisting of about 700 IJJs with a typical length of 300 μm are realized as mesa structures on top of BSCCO single crystals. An emission power P_e of up to 0.5 μW is detected for emission frequencies f_e between 0.5 and 0.8 THz. A lot of work has been performed following this discovery [4–48]; for a recent review, see Ref. [49]. P_e is raised to 82 μW with stand-alone structures, which are no longer patterned on a BSCCO base crystal [27,33]. By synchronizing three mesas patterned on the same base crystal, P_e is increased to 610 μW [30]. The linewidth of radiation can be as low as 6 MHz [44] and the maximum emission frequency reaches 1.6 THz [48]. In the IJJ stacks, THz emission is generated by the ac Josephson effect, yielding an emission frequency $f_e = 2eV_{\mathrm{dc}}/Nh$, where N is the number of junctions and V_{dc} is the total dc voltage across the stack. This relation assumes that the voltage drop V_{dc}/N is the same for all junctions. Furthermore, the Josephson relation suggests that f_e is freely tunable by the applied voltage (0.4836 THz per mV across each IJJ), perhaps up to the superconducting energy gap, which would yield a maximum emission frequency of some 10 THz. However, in real systems, there is strong Joule heating, leading, e.g., to the formation of hot spots (regions heated to temperatures above the critical temperature T_c) in the stack [7,13,14,29,31,36,43] and also limiting the maximum voltage per junction to values less than 3 mV. Furthermore, collective cavity modes utilizing the whole stack as a resonator seem to play an important role for synchronizing the IJJs [3,13,14].

Understanding—and ideally also controlling—the relations between THz emission, the inhomogeneous temperature distribution in the stack, and the mechanism of synchronization is a key issue in optimizing the device, not only with respect to P_e, f_e, and the linewidth of emission but also with respect to the tunability of both P_e and f_e. A series of papers addresses the issue of thermal management [6,17,24,40,41,45–48]. In particular, it is proposed that P_e can be enhanced by using a focused laser to locally increase the temperature variation in the stack, thereby strongly exciting plasma waves in the stack [41]. This method is used in the present work, although

*hbwang1000@gmail.com

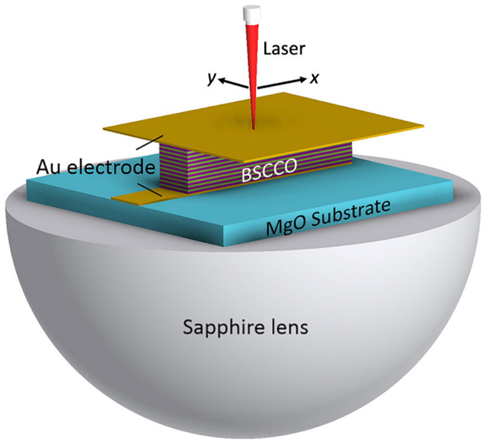

FIG. 1. Sketch of the GBG structure sample mounted on a hemispheric sapphire lens. A focused laser can scan across the sample surface while emission is detected through the lens by a Si bolometer (not shown in the sketch).

with the difference that, in Ref. [41], an initially homogeneous temperature distribution is assumed while, in our experiment, the sample investigated emits THz radiation in the presence of a hot spot. Measurements are done on an IJJ stack embedded between two gold layers, the gold-BSCCO-gold (GBG) structure [40]. By scanning the laser at half width along the length of the stack in the hot-spot regime, we succeed in changing P_e continuously at a constant bias current I. The variations in P_e are strongest when the laser is focused on a location where the local temperature in the stack roughly equals T_c.

Very recently, a similar experiment was performed using mesa structures. Also here, an increase of P_e is observed and appears when the hot-spot position is moved to a mesa end by locally heating the mesa surface with an 80 mW laser beam.

II. EXPERIMENTAL METHOD

A schematic diagram of the GBG structure is shown in Fig. 1. The lateral dimension of the sample studied in this work is about $290 \times 50\ \mu\mathrm{m}^2$. The sample is mounted on a hemispheric sapphire lens. A laser with wavelength $\lambda = 1310$ nm and a spot diameter of about 1 μm is focused onto the surface of the stack. The laser can scan across the surface of the stack with submicrometer precision. Using a Si bolometer, we measure the emission power of the sample from the other side of the hemispheric lens while keeping the laser on at the same time. The power detection and frequency measurement are similar to our previous work [14]. By modulating the laser power with a 10 kHz square signal and detecting the global differential voltage response ΔV of the stack with a lock-in technique while the sample is biased at a constant current, the setup can also be used as a low-temperature scanning laser microscope (LTSLM) [7,13,14,24]. In the present study, we use a comparatively strong beam power; thus, the LTSLM is operated in a manipulation mode rather than an imaging mode. In fact, we estimate that the maximum power of the laser beam arriving at the sample is in the range 2–5 mW. However, most of this intensity is reflected from the Au layer covering the mesa. From the change in the dc voltage across the stack upon laser irradiation, we estimate that a power of 100 μW or less (depending on the laser position and bias current) is absorbed by the mesa.

III. RESULTS AND DISCUSSIONS

In Fig. 2(a), the outermost branch of the current-voltage characteristic, at a bath temperature $T_b = 22$ K, is shown by a solid red line, and the emitted power, for the laser beam turned off, is presented in Fig. 2(b) as a function of bias current. Terahertz emission is only detected at the high-bias regime, from $(I, V_{\mathrm{dc}}) \sim (50\ \mathrm{mA}, 0.93\ \mathrm{V})$ to $\sim(20\ \mathrm{mA}, 0.88\ \mathrm{V})$. For the peak in P_e at $(I, V_{\mathrm{dc}}) = (28\ \mathrm{mA}, 0.883\ \mathrm{V})$, the emission frequency is found to be about 690 GHz, corresponding to $N \approx 620$ IJJs in the resistive state. By its color scale, Fig. 2(a) also shows the LTSLM signals $-\Delta V$ for a family of LTSLM linescans recorded for a large number of bias currents. The linescans are taken along the length of the stack at half of its width. In the graph, the two vertical dashed lines indicate the left and right boundaries of the stack. For currents below 20 mA, there is a strong signal near the left edge of the stack. This edge is not covered by the top Au layer and is much more sensitive to laser irradiation than other areas. One further observes that, near $I \approx 7$ mA, the strong LTSLM response extends significantly from the left edge of the stack toward the center of the stack. In this bias regime, where V_{dc} starts to bend back, a hot spot nucleates and is, presumably, to some extent, moved toward the interior of the stack by the laser beam during scanning. A similar effect (i.e., a laser-induced shift of the hot-spot position) is seen in Ref. [47]. For larger currents, $-\Delta V$ is more restricted to the left part of the stack and develops a local maximum inside the stack, which shifts to the right with increasing current (cf. the tilted, dashed line). This kind of maximum is typical for the edge of a hot spot [24]; i.e., we observe that, for currents above 12 mA, a stable hot spot forms in the left part of the stack and the hot spot increases in size with increasing current. In this regime, the reaction of the hot spot on the laser beam is close to the standard imaging mode; i.e., it slightly increases in size but its position remains fixed [24]. This seems natural because, with increasing dc input power, the relative contribution of the laser beam to local heat production becomes smaller.

Next, we investigate how P_e varies when the laser is positioned at different locations x_L along the stack. For the measurement, we place the laser at a given value x_L for 150 ms, measure P_e, and then vary x_L in steps of 1 μm. Figure 3(a) shows the resulting P_e vs x_L for $T_b = 22$ K and $I = 28$ mA. The lower horizontal dashed line in the graph

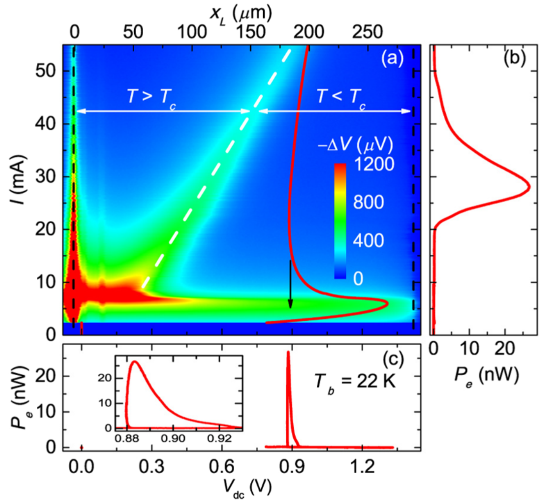

FIG. 2. For a bath temperature $T_b = 22$ K. (a) I-V characteristic (red line, bottom scale) and LTSLM signal $-\Delta V$ for a family of linescans along the length of the stack at half width, taken at different values of I (color scale). Graphs (b) and (c) show the emitted power P_e vs, respectively, I and V_{dc} when the laser is turned off. The inset in (c) shows P_e vs V_{dc} on an expanded voltage scale. The tilted dashed line in (a) separates regions where the stack temperature T is above (below) T_c. Vertical dashed lines indicate the edges of the stack.

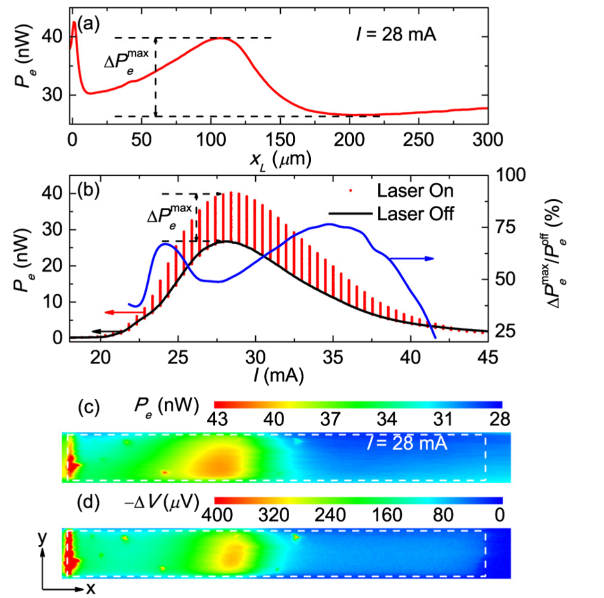

FIG. 3. (a) Emission power with laser positioned at coordinate x_L for a bias current of 28 mA. (b) P_e vs bias current while sweeping the laser, for discrete values of I, from $x_L = 10$ μm to $x_L = 300$ μm (left scale). The black line indicates P_e^{off} vs I, as measured for the laser turned off; thus, the vertical red lines indicate, for each current, the maximum laser-induced change $\Delta P_e^{\max}$. Right-hand scale, blue curve: ratio $\Delta P_e^{\max}/P_e^{\mathrm{off}}$ vs I. For $I = 28$ mA, (c) shows a 2D plot of P_e vs laser position (x_L, y_L) and (d) shows a 2D LTSLM image $-\Delta V$ vs (x_L, y_L). In (c) and (d), the boundaries of the stack are indicated by the dashed boxes. The bath temperature is 22 K.

indicates the emission power P_e^{off} when the laser is turned off. P_e varies from 26 nW to 42 nW when the laser is focused on the different locations of the sample. The largest emission power in the *interior* of the stack $P_e^{\max}$, indicated by the upper horizontal line in the graph, occurs for $x_L = 106$ μm, which in fact is close to the location where $-\Delta V$ has its local maximum [cf. Figs. 3(d) and 4(b)]. Figure 3(b) summarizes how P_e varies with I: for each current (step width $\Delta I = 0.5$ mA), the laser is scanned from $x_L = 10$ μm to $x_L = 300$ μm; i.e., we exclude the strong signal from the left edge for this measurement. In the graph, we also plot by a black line P_e^{off} vs I, as measured when the laser is turned off; thus, the vertical red lines indicate for each current the maximum laser-induced change $\Delta P_e^{\max}$. The normalized ratio $\Delta P_e^{\max}/P_e^{\mathrm{off}}$ is shown by the blue curve in Fig. 3(b), referring to the right axis of this graph. As can be seen, the emission power is enhanced for almost every bias current and $\Delta P_e^{\max}/P_e^{\mathrm{off}}$ reaches values between 50% and 80% for currents between 23 mA and 39 mA. For $I = 28$ mA and $T_b = 22$ K, Fig. 3(c) shows how P_e varies when the laser is scanned both along the x and y directions. There is a hot zone at the left edge of the stack and another hot zone near $x_L = 100$ μm. For comparison, Fig. 3(d) shows the 2D LTSLM image $-\Delta V$ vs laser position (x_L, y_L). One notes that the two images are very similar, leading to the suspicion that the laser-induced change ΔP_e in emission power is (almost) proportional to the laser-induced voltage change ΔV, independent of the laser position.

To study this further, we compare, in Fig. 4, for $T_b = 22$ K and four selected bias currents, (a) the laser-induced change in dc voltage $-\Delta V_{\mathrm{dc}}$, (b) the LTSLM signal $-\Delta V$, and (c) the laser-induced change ΔP_e in emission power. Note that ΔV_{dc} and ΔV would be the same if the laser is modulated arbitrarily slowly, rather than with 10 kHz. For measuring ΔV_{dc} (and ΔP_e), the laser, while still modulated, is kept at a fixed position x_L for 150 ms. Thus, ΔV_{dc} measures laser-induced temperature changes which occur within 150 ms of (modulated) laser irradiation while ΔV gives the short time response. Not very surprisingly, the overall amplitude of ΔV_{dc} is larger than the amplitude of ΔV and the positions of the minima (the hot-spot edges) are slightly shifted to the left for ΔV_{dc} compared to ΔV. More importantly, the shape of $-\Delta V$ vs x_L is basically the same as the shape of ΔP_e vs x_L. In Fig. 4(d), we plot ΔP_e vs $-\Delta V_{\mathrm{dc}}$ for the four bias currents and all values of x_L; i.e., x_L runs as a parameter in this graph. In the plot, we exclude the data from the edge peak, because here the time delay of the Si bolometer relative to the voltmeter causes a significant phase shift between ΔP_e and ΔV_{dc}. For the rest of the x_L values, one obtains straight lines for all currents, confirming the proportionality of ΔP_e and ΔV_{dc}. Note that the slopes $\Delta P_e/\Delta V_{\mathrm{dc}}$ amount to about -3 nW/mV for

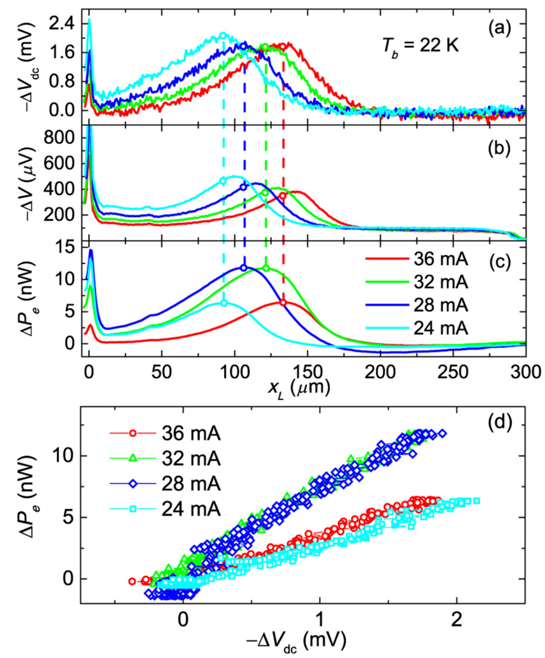

FIG. 4. Four linescans of the laser along the width of the stack. (a) Global laser-induced change in the dc voltage $-\Delta V_{\mathrm{dc}}$ across the stack, (b) LTSLM signal $-\Delta V$, and (c) change in emission power ΔP_e vs coordinate x_L on the scanning line. (d) Plot of ΔP_e vs $-\Delta V_{\mathrm{dc}}$ for laser positioned from $x_L = 10\ \mu$m to 300 μm.

bias currents of, respectively, 24 mA and 36 mA and to about -6 nW/mV for bias currents 28 mA and 32 mA. The large values of $|\Delta P_e/\Delta V_{\mathrm{dc}}|$ are in fact obtained near the center of the emission peak in P_e vs, respectively, I and V_{dc}; cf. Figs. 2(b), 2(c), and 3(b).

The proportionality $\Delta P_e \propto \Delta V_{\mathrm{dc}}$ is unexpected. In view of the proposal of Ref. [41], one might assume that there is a big difference if the laser is positioned inside the hot-spot region compared to a position where the stack temperature is below T_c. Furthermore, when the laser is positioned near the edges of the stack, the local electric and magnetic field distribution, and thus the radiation impedance [15], might change, giving rise to a change in $P_e(x_L, y_L)$. In particular, one would expect signals in Fig. 3(c) or in Fig. 4(c) on the cold edge of the stack. This is not observed. For the experiments described in Ref. [47], performed on mesa structures, it is concluded that the laser-induced enhancement of the emission power is realized by an adjustment of the hot-spot position. Also for this case, we do not see a reason why $P_e(x_L, y_L)$ and $\Delta V(x_L, y_L)$ should be strictly proportional to each other.

Accepting the proportionality of ΔP_e to the global response ΔV_{dc}, one might assume that by changing V_{dc} with the amount ΔV_{dc}, one simply moves toward a lower voltage in the P_e vs V_{dc} curve of Fig. 2(c). However, the bias currents in Fig. 4 are chosen so that in P_e vs V_{dc} points on both sides of the emission peak are covered; thus, one should get different signs of the response, e.g., for $I = 24$ mA and 36 mA. With the laser turned on, there is also a slight increase in the average stack temperature which to some extent is equivalent to an increase of the bath temperature. For the sample, we find that, for the bias currents of interest, V_{dc} changes by about 3–4 mV/K. Thus, the laser-induced relative change in voltage corresponds to a change in T_b of about 0.2 K. By changing T_b for fixed values of the bias current, we find that P_e in fact oscillates as a function ΔV_{dc} and, near the bath temperature of 22 K, increases by more than a factor of 5 when increasing T_b by only 2 K. A 0.2 K laser-induced temperature change is thus compatible with the increase in P_e that we observe.

IV. SUMMARY

In summary, we investigate the response of a BSCCO intrinsic Josephson-junction stack, embedded between two gold electrodes, to a focused laser beam which is scanned across the stack. The laser-induced changes in the voltage V_{dc} across the stack and in the THz emission power P_e are measured simultaneously. The study is motivated by the recent theoretical study [41] proposing that a laser beam locally heating the stack, thereby causing a critical current inhomogeneity, can give rise to a strong enhancement of P_e in comparison with the homogeneous state. In our experiment, the sample does not emit in the low-bias regime, neither in the absence nor in the presence of the laser beam. However, the laser-induced changes of the emission power are found at the high-bias regime in the presence of a hot spot. For a bath temperature near 22 K, the laser-induced changes $\Delta P_e(x_L, y_L)$ are proportional to the voltage change $\Delta V_{\mathrm{dc}}(x_L, y_L)$ for all values of the position (x_L, y_L) of the laser beam. $\Delta V_{\mathrm{dc}}(x_L, y_L)$ itself, and consequently also $\Delta P_e(x_L, y_L)$, strongly depends on the (x_L, y_L) position, being, e.g., large near the edge of the hot spot. The laser-induced change of the voltage across the stack is essentially determined by the temperature dependence of the BSCCO c-axis conductance, as is analyzed in Ref. [24]. In fact, we would have expected that different mechanisms lead to laser-induced changes of the emission power, in which case $\Delta P_e(x_L, y_L)$ and $\Delta V_{\mathrm{dc}}(x_L, y_L)$ should have different dependences on the local beam position. The unexpected *global* response is likely to be related to a change in the *average* stack temperature and is consistent with the change in P_e when increasing the bath temperature by about 0.2 K.

ACKNOWLEDGMENTS

We gratefully acknowledge financial support by the National Natural Science Foundation of China (Grant No. 11234006), the Priority Academic Program Development of Jiangsu Higher Education Institutions, the Deutsche Forschungsgemeinschaft (Project No. KL930/12-1), the Grants-in-Aid for Scientific

Research from JSPS (No. 25289108), and RFBR Grants No. 13-02-00493-a and No. 14-02-91335, and Ministry of Education and Science of the Russian Federation Grant No. 14.607.21.0100.

[1] B. Ferguson and X. C. Zhang, Materials for terahertz science and technology, Nat. Mater. **1**, 26 (2002).
[2] M. Tonouchi, Cutting-edge terahertz technology, Nat. Photonics **1**, 97 (2007).
[3] L. Ozyuzer, A. E. Koshelev, C. Kurter, N. Gopalsami, Q. Li, M. Tachiki, K. Kadowaki, T. Yamamoto, H. Minami, H. Yamaguchi, T. Tachiki, K. E. Gray, W.-K. Kwok, and U. Welp, Emission of coherent THz radiation from superconductors, Science **318**, 1291 (2007).
[4] S. Z. Lin and X. Hu, Possible Dynamic States in Inductively Coupled Intrinsic Josephson Junctions of Layered High-T_c Superconductors, Phys. Rev. Lett. **100**, 247006 (2008).
[5] A. E. Koshelev, Alternating dynamic state self-generated by internal resonance in stacks of intrinsic Josephson junctions, Phys. Rev. B **78**, 174509 (2008).
[6] C. Kurter, K. E. Gray, J. F. Zasadzinski, L. Ozyuzer, A. E. Koshelev, Q. Li, T. Yamamoto, K. Kadowaki, W.-K. Kwok, M. Tachiki, and U. Welp, Thermal management in large Bi2212 mesas used for terahertz sources, IEEE Trans. Appl. Supercond. **19**, 428 (2009).
[7] H. B. Wang, S. Guénon, J. Yuan, A. Iishi, S. Arisawa, T. Hatano, T. Yamashita, D. Koelle, and R. Kleiner, Hot Spots and Waves in $Bi_2Sr_2CaCu_2O_8$ Intrinsic Josephson Junction Stacks: A Study by Low Temperature Scanning Laser Microscopy, Phys. Rev. Lett. **102**, 017006 (2009).
[8] M. Tachiki, S. Fukuya, and T. Koyama, Mechanism of Terahertz Electromagnetic Wave Emission from Intrinsic Josephson Junctions, Phys. Rev. Lett. **102**, 127002 (2009).
[9] N. F. Pedersen and S. Madsen, THz generation using fluxon dynamics in high temperature superconductors, IEEE Trans Appl. Supercond. **19**, 726 (2009).
[10] A. E. Koshelev, Stability of dynamic coherent states in intrinsic Josephson-junction stacks near internal cavity resonance, Phys. Rev. B **82**, 174512 (2010).
[11] S. Z. Lin and X. Hu, Response and amplification of terahertz electromagnetic waves in intrinsic Josephson junctions of layered high-T_c superconductor, Phys. Rev. B **82**, 020504 (2010).
[12] M. Tsujimoto, K. Yamaki, K. Deguchi, T. Yamamoto, T. Kashiwagi, H. Minami, M. Tachiki, K. Kadowaki, and R. A. Klemm, Geometrical Resonance Conditions for THz Radiation from the Intrinsic Josephson Junctions in $Bi_2Sr_2CaCu_2O_{8+\delta}$, Phys. Rev. Lett. **105**, 037005 (2010).
[13] H. B. Wang, S. Guénon, B. Gross, J. Yuan, Z. G. Jiang, Y. Y. Zhong, M. Grünzweig, A. Iishi, P. H. Wu, T. Hatano, D. Koelle, and R. Kleiner, Coherent Terahertz Emission of Intrinsic Josephson Junction Stacks in the Hot Spot Regime, Phys. Rev. Lett. **105**, 057002 (2010).
[14] S. Guénon, M. Grünzweig, B. Gross, J. Yuan, Z. G. Jiang, Y. Y. Zhong, M. Y. Li, A. Iishi, P. H. Wu, T. Hatano, R. G. Mints, E. Goldobin, D. Koelle, H. B. Wang, and R. Kleiner, Interaction of hot spots and terahertz waves in $Bi_2Sr_2CaCu_2O_8$ intrinsic Josephson junction stacks of various geometry, Phys. Rev. B **82**, 214506 (2010).
[15] V. M. Krasnov, Coherent flux-flow emission from stacked Josephson junctions: Nonlocal radiative boundary conditions and the role of geometrical resonances, Phys. Rev. B **82**, 134524 (2010).
[16] V. M. Krasnov, Terahertz electromagnetic radiation from intrinsic Josephson junctions at zero magnetic field via breather-type self-oscillations, Phys. Rev. B **83**, 174517 (2011).
[17] A. Yurgens, Temperature distribution in a large $Bi_2Sr_2CaCu_2O_{8+\delta}$ mesa, Phys. Rev. B **83**, 184501 (2011).
[18] T. M. Benseman, A. E. Koshelev, K. E. Gray, W.-K. Kwok, U. Welp, K. Kadowaki, M. Tachiki, and T. Yamamoto, Tunable terahertz emission from $Bi_2Sr_2CaCu_2O_{8+\delta}$ mesa devices, Phys. Rev. B **84**, 064523 (2011).
[19] T. Koyama, H. Matsumoto, M. Machida, and Y. Ota, Multiscale simulation for terahertz wave emission from the intrinsic Josephson junctions, Supercond. Sci. Technol. **24**, 085007 (2011).
[20] M. Tsujimoto, H. Minami, K. Delfanazari, M. Sawamura, R. Nakayama, T. Kitamura, T. Yamamoto, T. Kashiwagi, T. Hattori, and K. Kadowaki, Terahertz imaging system using high-T_c superconducting oscillation devices, J. Appl. Phys. **111**, 123111 (2012).
[21] S. Z. Lin and X. Hu, In-plane dissipation as a possible synchronization mechanism for terahertz radiation from intrinsic Josephson junctions of layered superconductors, Phys. Rev. B **86**, 054506 (2012).
[22] M. Y. Li, J. Yuan, N. V. Kinev, J. Li, B. Gross, S. Guénon, A. Ishii, K. Hirata, T. Hatano, D. Koelle, R. Kleiner, V. P. Koshelets, H. B. Wang, and P. H. Wu, Linewidth dependence of coherent terahertz emission from $Bi_2Sr_2CaCu_2O_8$ intrinsic Josephson junction stacks in the hot-spot regime, Phys. Rev. B **86**, 060505(R) (2012).
[23] I. Kakeya, Y. Omukai, T. Yamamoto, K. Kadowaki, and M. Suzuki, Effect of thermal inhomogeneity for terahertz radiation from intrinsic Josephson junction stacks of $Bi_2Sr_2CaCu_2O_{8+\delta}$, Appl. Phys. Lett. **100**, 242603 (2012).
[24] B. Gross, S. Guénon, J. Yuan, M. Y. Li, J. Li, A. Ishii, R. G. Mints, T. Hatano, P. H. Wu, D. Koelle, H. B. Wang, and R. Kleiner, Hot-spot formation in stacks of intrinsic Josephson junctions in $Bi_2Sr_2CaCu_2O_8$, Phys. Rev. B **86**, 094524 (2012).
[25] J. Yuan, M. Y. Li, J. Li, B. Gross, A. Ishii, K. Yamaura, T. Hatano, K. Hirata, E. Takayama-Muromachi, P. H. Wu, D. Koelle, R. Kleiner, and H. B. Wang, Terahertz emission from $Bi_2Sr_2CaCu_2O_8$ intrinsic Josephson junction stacks with all-superconducting electrodes, Supercond. Sci. Technol. **25**, 075015 (2012).
[26] T. Kashiwagi, M. Tsujimoto, T. Yamamoto, H. Minami, K. Yamaki, K. Delfanazari, K. Deguchi, N. Orita, T. Koike, R. Nakayama, T. Kitamura, M. Sawamura, S. Hagino, K. Ishida, K. Ivanovic, H. Asai, M. Tachiki, R. A. Klemm, and K. Kadowaki, High temperature superconductor terahertz emitters: Fundamental physics and its applications, J. Appl. Phys. **51**, 010113 (2012).
[27] S. Sekimoto, C. Watanabe, H. Minami, T. Yamamoto, T. Kashiwagi, R. A. Klemm, and K. Kadowaki, Continuous

30 μW terahertz source by a high-T_c superconductor mesa structure, Appl. Phys. Lett. **103**, 182601 (2013).
[28] I. Kawayama, C. H. Zhang, H. B. Wang, and M. Tonouchi, Study on terahertz emission and optical/terahertz pulse responses with superconductors, Supercond. Sci. Technol. **26**, 093002 (2013).
[29] T. M. Benseman, A. E. Koshelev, W.-K. Kwok, U. Welp, K. Kadowaki, J. R. Cooper, and G. Balakrishnan, The ac Josephson relation and inhomogeneous temperature distributions in large $Bi_2Sr_2CaCu_2O_{8+\delta}$ mesas for THz emission, Supercond. Sci. Technol. **26**, 085016 (2013).
[30] T. M. Benseman, K. E. Gray, A. E. Koshelev, W.-K. Kwok, U. Welp, H. Minami, K. Kadowaki, and T. Yamamoto, Powerful terahertz emission from $Bi_2Sr_2CaCu_2O_{8+\delta}$ mesa arrays, Appl. Phys. Lett. **103**, 022602 (2013).
[31] T. M. Benseman, A. E. Koshelev, W.-K. Kwok, U. Welp, V. K. Vlasko-Vlasov, K. Kadowaki, H. Minami, and C. Watanabe, Direct imaging of hot spots in $Bi_2Sr_2CaCu_2O_{8+\delta}$ mesa terahertz sources, J. Appl. Phys. **113**, 133902 (2013).
[32] B. Gross, J. Yuan, D. Y. An, M. Y. Li, N. V. Kinev, X. J. Zhou, M. Ji, Y. Huang, T. Hatano, R. G. Mints, V. P. Koshelets, P. H. Wu, H. B. Wang, D. Koelle, and R. Kleiner, Modeling the linewidth dependence of coherent terahertz emission from intrinsic Josephson junction stacks in the hot-spot regime, Phys. Rev. B **88**, 014524 (2013).
[33] D. Y. An, J. Yuan, N. V. Kinev, M. Y. Li, Y. Huang, M. Ji, H. Zhang, Z. L. Sun, L. Kang, B. B. Jin, J. Chen, J. Li, B. Gross, A. Ishii, K. Hirata, T. Hatano, V. P. Koshelets, D. Koelle, R. Kleiner, H. B. Wang, W. W. Xu, and P. H. Wu, Terahertz emission and detection both based on high-T_c superconductors: Towards an integrated receiver, Appl. Phys. Lett. **102**, 092601 (2013).
[34] F. Turkoglu, L. Ozyuzer, H. Koseoglu, Y. Demirhan, S. Preu, S. Malzer, Y. Simsek, H. B. Wang, and P. Müller, Emission of the THz waves from large area mesas of superconducting $Bi_2Sr_2CaCu_2O_8$ by the injection of spin polarized current, Physica (Amsterdam) C **491**, 7 (2013).
[35] K. Kadowaki, M. Tsujimoto, K. Delfanazari, T. Kitamura, M. Sawamura, H. Asai, T. Yamamoto, K. Ishida, C. Watanabe, and S. Sekimoto, Quantum terahertz electronics (QTE) using coherent radiation from high temperature superconducting $Bi_2Sr_2CaCu_2O_8$ intrinsic Josephson junctions, Physica (Amsterdam) C **491**, 2 (2013).
[36] H. Minami, C. Watanabe, K. Sato, S. Sekimoto, T. Yamamoto, T. Kashiwagi, R. A. Klemm, and K. Kadowaki, Local SiC photoluminescence evidence of hot spot formation and sub-THz coherent emission from a rectangular $Bi_2Sr_2CaCu_2O_{8+\delta}$ mesa, Phys. Rev. B **89**, 054503 (2014).
[37] T. Kashiwagi, K. Nakade, B. Markovic, Y. Saiwai, H. Minami, T. Kitamura, C. Watanabe, K. Ishida, S. Sekimoto, K. Asanuma, T. Yasui, Y. Shibano, M. Tsujimoto, T. Yamamoto, J. Mirkovic, and K. Kadowaki, Reflection type of terahertz imaging system using a high-T_c superconducting oscillator, Appl. Phys. Lett. **104**, 022601 (2014).
[38] T. Kashiwagi, K. Nakade, Y. Saiwai, H. Minami, T. Kitamura, C. Watanabe, K. Ishida, S. Sekimoto, K. Asanuma, T. Yasui, Y. Shibano, M. Tsujimoto, T. Yamamoto, B. Markovic, J. Mirkovic, R. A. Klemm, and K. Kadowaki, Computed tomography image using sub-terahertz waves generated from a high-T_c superconducting intrinsic Josephson junction oscillator, Appl. Phys. Lett. **104**, 082603 (2014).
[39] A. Grib and P. Seidel, The influence of external separate heating on the synchronization of Josephson junctions, Phys. Status Solidi B **251**, 1040 (2014).
[40] M. Ji, J. Yuan, B. Gross, F. Rudau, D. Y. An, M. Y. Li, X. J. Zhou, Y. Huang, H. C. Sun, Q. Zhu, J. Li, N. Kinev, T. Hatano, V. P. Koshelets, D. Koelle, R. Kleiner, W. W. Xu, B. B. Jin, H. B. Wang, and P. H. Wu, $Bi_2Sr_2CaCu_2O_8$ intrinsic Josephson junction stacks with improved cooling: Coherent emission above 1 THz, Appl. Phys. Lett. **105**, 122602 (2014).
[41] H. Asai and S. Kawabata, Intense terahertz emission from intrinsic Josephson junctions by external heat control, Appl. Phys. Lett. **104**, 112601 (2014).
[42] T. Kitamura, T. Kashiwagi, T. Yamamoto, M. Tsujimoto, C. Watanabe, K. Ishida, S. Sekimoto, K. Asanuma, T. Yasui, K. Nakade, Y. Shibano, Y. Saiwai, H. Minami, R. A. Klemm, and K. Kadowaki, Broadly tunable, high-power terahertz radiation up to 73 K from a stand-alone $Bi_2Sr_2CaCu_2O_{8+\delta}$ mesa, Appl. Phys. Lett. **105**, 202603 (2014).
[43] M. Tsujimoto, H. Kambara, Y. Maeda, Y. Yoshioka, Y. Nakagawa, and I. Kakeya, Dynamic control of temperature distributions in stacks of intrinsic Josephson junctions in $Bi_2Sr_2CaCu_2O_{8+\delta}$ for intense terahertz radiation, Phys. Rev. Appl. **2**, 044016 (2014).
[44] H. B. Wang, M. Y. Li, J. Yuan, N. Kinev, J. Li, B. Gross, S. Guénon, A. Ishii, T. Hatano, D. Koelle, R. Kleiner, V. P. Koshelets, and P. H. Wu, in *IEEE Proceedings of the 37th International Conference on Infrared, Millimeter, and Terahertz Waves* (IEEE, New York, 2012).
[45] A. Yurgens and L. N. Bulaevskii, Temperature distribution in a stack of intrinsic Josephson junctions with their CuO-plane electrodes oriented perpendicular to supporting substrate, Supercond. Sci. Technol. **24**, 015003 (2011).
[46] H. Asai, M. Tachiki, and K. Kadowaki, Three-dimensional numerical analysis of terahertz radiation emitted from intrinsic Josephson junctions with hot spots, Phys. Rev. B **85**, 064521 (2012).
[47] C. Watanabe, H. Minami, T. Kitamura, K. Asanuma, K. Nakade, T. Yasui, Y. Saiwai, Y. Shibano, T. Yamamoto, T. Kashiwagi, R. A. Klemm, and K. Kadowaki, Influence of the local heating position on the terahertz emission power from high-T_c superconducting $Bi_2Sr_2CaCu_2O_{8+\delta}$ mesas, Appl. Phys. Lett. **106**, 042603 (2015).
[48] T. Kashiwagi, T. Yamamoto, T. Kitamura, K. Asanuma, C. Watanabe, K. Nakade, T. Yasui, Y. Saiwai, Y. Shibano, H. Kubo, K. Sakamoto, T. Katsuragawa, M. Tsujimoto, K. Delfanazari, R. Yoshizaki, H. Minami, R. A. Klemm, and K. Kadowaki, Generation of electromagnetic waves from 0.3 to 1.6 terahertz with a high-T_c superconducting $Bi_2Sr_2CaCu_2O_{8+\delta}$ intrinsic Josephson junction emitter, Appl. Phys. Lett. **106**, 092601 (2015).
[49] U. Welp, K. Kadowaki, and R. Kleiner, Superconducting emitters of THz radiation, Nat. Photonics **7**, 702 (2013).